A Design and Dispatch Optimization Algorithm based on Mixed Integer Linear Programming for Rural Electrification

L. Moretti, M. Astolfi, C.Vergara, E. Macchi, J. I. Pérez-Arriaga, G. Manzolini

Abstract

Off-grid microgrids constitute an increasingly viable alternative to grid extension for rural electrification. Thanks to significant reductions in hardware cost, energy cost for off-grid users in areas sparsely covered by the national grid has become competitive with grid-connection once infrastructural costs are accounted for. Microgrids offer advantages also from an environmental and social point of view, featuring generation systems with high renewable penetration and facilitating the involvement of local communities in development projects. To further enhance microgrids economic competitiveness, it is necessary to devise innovative control strategies and design algorithms, that can ensure an optimal operating performance at the lowest overall cost. In this paper we present a new predictive design and dispatch optimization algorithm based on Mixed Integer Linear Programming (MILP). The new method is compared to a previously developed heuristic methodology, applying both to the design and yearly performance estimation of local microgrids, characterized on the basis of real data relative to a sub-Saharan African region. The potential advantages of including the proposed microgrid design method in a regional electrification planning model are illustrated in a realistic case example.

1. Introduction

Access to affordable electricity supply is widely viewed as a key requirement to drive human development and diminish poverty levels worldwide. For this reason, the United Nations have set as part of the 2030 Agenda for Sustainable Development the ambitious goal of reaching universal energy access by 2030 [1]. Local governments and regulators in many developing countries, supported by international cooperation agencies, are therefore working on programs to extend energy access for the population in a cost-effective manner [2].
At the same time, in the last decade, the technological cost to supply rural communities through local renewable energy sources (RES) such as wind and photovoltaic has dramatically dropped [3], making off-grid systems an increasingly attractive alternative to grid extension [4]. In many cases, microgrids and standalone systems have the potential to be a cost-effective solution to provide electricity access in areas sparsely covered by the national grid. Furthermore, they constitute the only viable electrification strategy for remote communities, which would otherwise unlikely be included in grid extension plans [5]. The national grid still offers electricity at a cheaper price than installing and operating an off-grid system, but its extension involves relevant costs for erecting new transmission lines and, in developing countries, is a solution that generally suffers from large transmission losses and a poor reliability [6]. On the contrary, microgrids have the potential to allow for a high penetration of renewable sources, contributing to lower the environmental impact of the energy consumption from new customers, and put the basis for the growth of a national electric system which is both economically [7] and environmentally [8] sustainable.

Microgrids need substantial investments in the distribution network infrastructure, but also exhibit economies of scale as the energy demand served increases, making clustering of neighboring users within a single microgrid a potential strategy to lower energy cost [9].

To ensure the competitiveness of off-grid systems, a critical stage is sizing components and defining an effective operation strategy, so to minimize the levelized cost of electricity (LCOE) for its users. Different approaches can be followed as summarized in table 1.

Table 1 – brief classification of the approaches available in literature for the microgrid design optimization

Model type	Design identification (layer 1)	Dispatch strategy (layer 2)	
Analytical	Analytical expression	Simulation not performed	
two-layers	Grid search (GA, PSO, Pattern Search)	Heuristic	LF
			CC
			ABV
		MILP	
single layer	MILP		

Off-grid LCOE can be estimated using *analytical models* that do not simulate the system operation over a period but only require assumptions on overall energy demand and technological performances of components [10], or that include also additional lumped factors, such as population density [11]. These models present the advantage of requiring very short computation time, and for this reason they are the preferred method for off-grid cost estimate in preliminary electrification planning studies. On the other hand, they do not explicitly address the design and dispatch problem, which can lead to a misleading LCOE estimate. This limitation can be overcome with more complex simulation-based design algorithms that select the size of components based on the simulated performance of candidate solutions over a reference period.

A broad range of different *two-layers models* have been proposed in literature [12]. Most of the approaches decouple design and dispatch problems, resorting to the performance evaluation of fixed architecture systems as fitness parameter to guide the exploration of the design space [13]. Adopting heuristic dispatch logics is a fast and realistic way of simulating the microgrid operation. They comprise of a set of predetermined rules that control the system based on its status and on the characteristics of the installed equipment and have the merit of being easily deployable in real systems given the state of the art in commercially available hardware. They are implemented in the widely known simulation-based microgrid design optimization software HOMER [14], which features Cycle-Charging (CC) and Load Following (LF). Alternative strategies to the ones used by HOMER are evaluated by Li [15]: among them, the Advanced Battery Valuation (ABV) strategy attains a good performance without equipment oversizing, and does not required the calibration of the diesel activation/deactivation threshold used by the CC approach. More advanced second-layer control strategies, suited for complicated system architectures, can rely on Mixed Integer Linear Programming. [16] The MILP formulation makes use of effective mathematical algorithms to identify the optimal solution taking advantage of future expected behavior of exogenous factors (like load and solar radiation) to reduce operating costs. Formal set points optimization can lead to remarkable savings with respect to simpler heuristic strategies, as shown by Mazzola et al. [17] for a rural ICE-BESS-PV microgrid.

As drawback, the two-layers models complicate the introduction of seasonal and yearly constraints: the fitness of design solutions that do not enforce the requirements on overall system performance can be penalized, but the structure of their operational behavior cannot be modified to try and impose them. Furthermore, an accurate accounting of wearing cost for components whose lifetime is influenced by their yearly dispatch requires an iterative procedure.

Integrating the optimization of design and dispatch in a *single layer model* leads to the formulation of a complex problem, that can be tackled via MILP. The most famous software for design optimization relying on this technique is DER-CAM [18], developed at Lawrence Berkeley National Laboratory since early 2000. The software is oriented towards design and operation evaluation for complex CHP and trigenerative grid-connected microgrids in developed countries and includes the evaluation of the thermal behavior of buildings.

A much simpler model is presented by Ferrer-Martí [19] for the optimization of spatially distributed off-grid microgrids featuring solar panels and wind turbine generators. The model optimizes number and location of installed units and electrical connections between consumption points but does not consider the installation and management of dispatchable generators. In [20] the design of a distributed multi-node CHP system featuring dispatchable and

non-dispatchable DERs is optimized via a MILP in both on-grid and off-grid scenarios. Although partial load operation is allowed for dispatchable units, a constant efficiency is assumed for the machines. The effect of components wearing on their lifetime is also not accounted for. The model does not deal with the non-deterministic nature of renewable energy production, nor performs a re-evaluation of the microgrid performance with limited future foresight.

The three main contributions of this work are:

1- To propose a new MILP formulation for the optimal design of microgrids with discrete catalogue-based components selection. An explicit dependency of annuitized investment cost for engines and batteries on their operation is also introduced. The algorithm is suitable for general rural off-grid systems design and allows for the effective inclusion of aggregate operation constraints in the design stage.
2- To propose a framework to evaluate investment and operation algorithms from the local and regional viewpoints. The yearly operation of the optimal system is evaluated adopting a Rolling Horizon (RH) approach, via a realistic day-ahead MILP-based dispatch optimization. The performance of the new predictive algorithm is compared to the Advanced Battery Valuation (ABV) strategy described in [15], performing design and operation evaluation for a large number of rural microgrids of different sizes, assuming a deployment in sub-Saharan African regions.
3- To illustrate the importance of improved operation and design of microgrids when they are inserted in regional electrification planning processes. The impact can be both in terms of the cost and the mix of electrification modes. The regional analysis is carried out with a preliminary and simplified version of the electrification algorithm described in [21].

2. Reference context

Results presented in this paper refer to a test case representative of a rural region in sub-Saharan Africa[1]. The information required to characterize the region includes its topography, the layout of the existing national grid and the characterization of non-electrified customers. The topography of the region was obtained from a publicly available database (NASA Shuttle Radar Topography Mission [22]). The location and typology of the buildings was obtained from a prior electrification study, which made use of satellite imagery. Layout and technical characteristics of the main grid up to medium voltage (MV) was provided by the same source. Figure 1 depicts the test case region and the layout of the existing MV grid. The buildings with a distance smaller than 500 m from the main grid have been considered as already grid connected, and thus excluded from the analysis. The characterization of hourly patterns of electricity usage for ten categories of users is based on a dataset provided by members of the MIT / Comillas Universal Energy Access Lab[2], featuring the results of a field survey. The methodology adopted in reconstructing the energy consumption profiles is described in [15]. Table 2 shows the building types and the number for each type present within the region. Each type is characterized by a list of appliances that are most likely to be acquired once electric energy becomes available. Starting from the rated power of each appliance, verbal descriptions of its usage pattern and considering an aleatory variation respect to the average profile, a library of different reference energy consumption profiles for each customer type has been produced. Examples of class-specific profiles are shown in Figure 2 for six different types of users. The black lines represent the annual average hourly load profiles while the two red dotted lines are the 5^{th} and 95^{th} percentiles, respectively.

[1] Due to the existence of a non-disclosure agreement between the author's institution and the local distribution and transmission authority providing the dataset, the exact location of the region adopted as case study is not declared here.
[2] See http://universalaccess.mit.edu

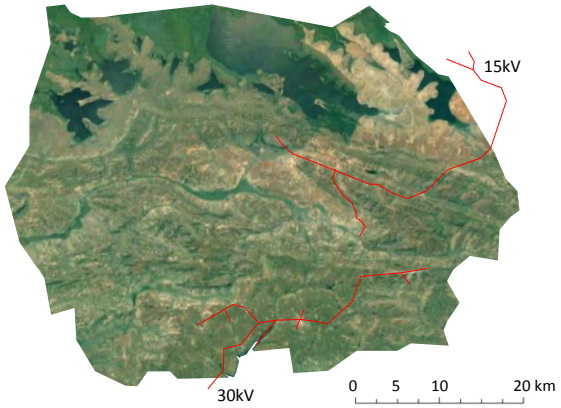

Figure 1: test case region map, with identification of existing national 30 kV and 15 kV grids

Total number of buildings			47251
Estimated number of currently electrified buildings			6435
Numbers of non-electrified buildings			
Small residential	31879	Cooperatives	55
Large residential	7967	Government	8
Shops	768	Primary school	31
Banks	43	Secondary school	20
Churches	40	Hospitals	5

Table 2: test case consumers by type in the considered region

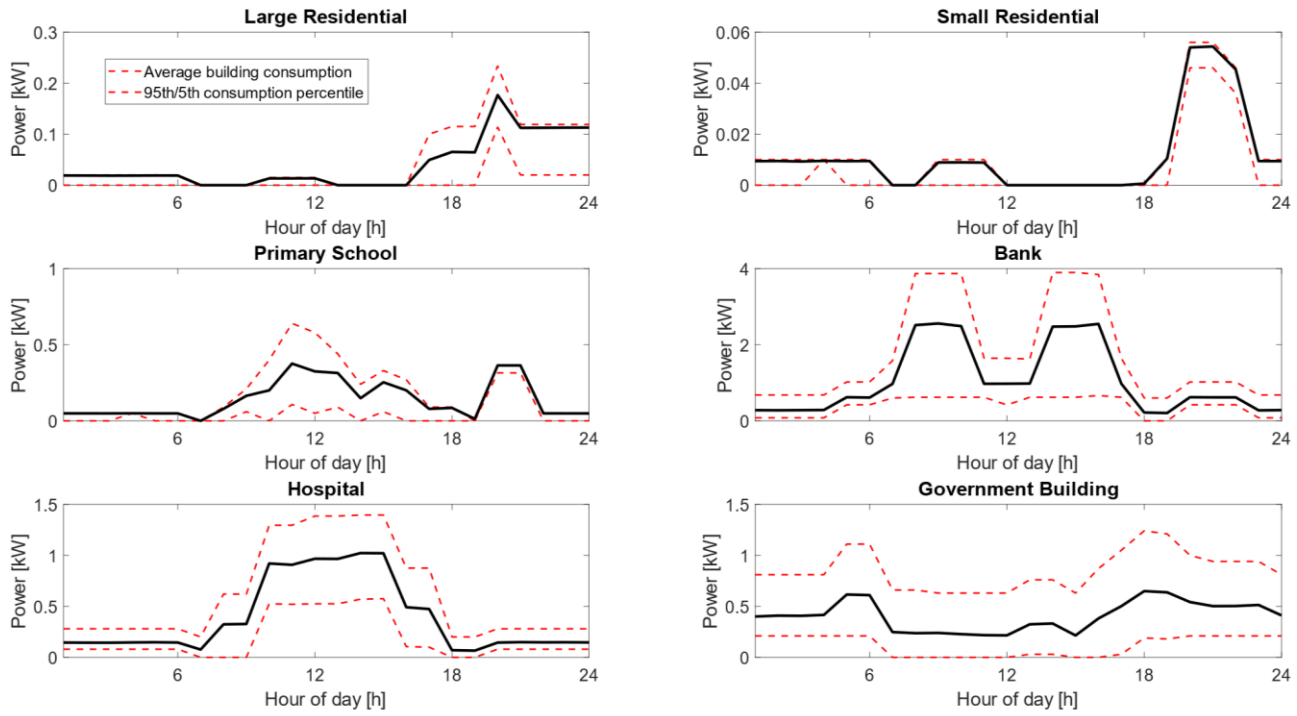

Figure 2: average consumption profile and hourly load variability for different types of users

3. Microgrid architecture

The microgrid architecture shown in Figure 3 is adopted throughout the present work [23]. A photovoltaic (PV) array and a battery energy storage system (BESS) are connected to a direct current (DC) bus, which can bi-directionally exchange energy with an alternate current (AC) bus via an inverter/rectifier. The loads and an internal combustion engine (ICE) are directly connected to the AC bus. Network losses are only considered in the delivery from the AC bus to the load, through an average loss coefficient; network losses between the generation and storage units are neglected as the components are assumed to be close to one another. The efficiencies of the PV array charge controller and of the inverter/rectifier are also accounted for.

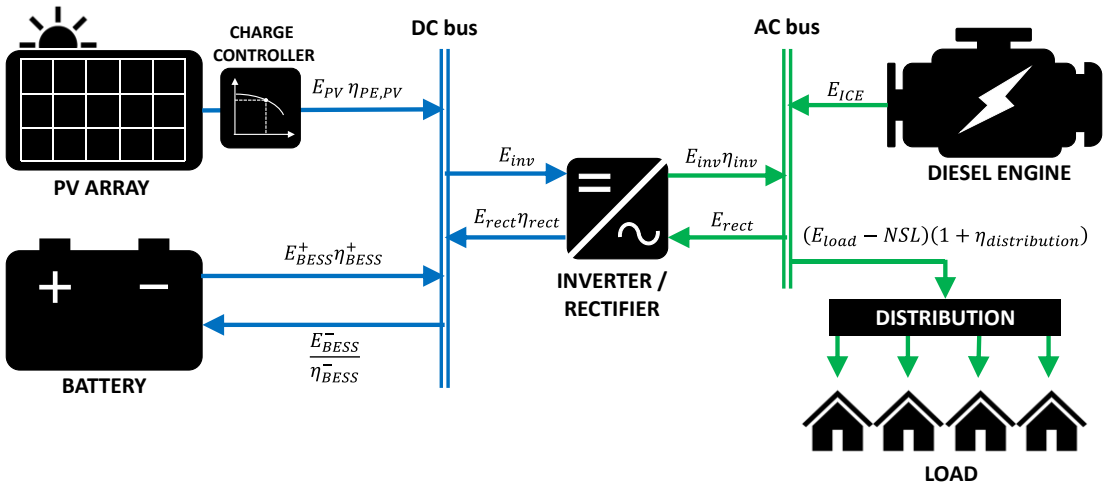

Figure 3: microgrid architecture

The objective of the design optimization is to minimize the sum of the annuitized investment and operation costs (*annuity*) to electrify a given group of users, which are represented by their aggregate hourly consumption profile. The optimal design defines size, number and typology of the components to be installed.
Two energy balances are imposed on the AC and DC buses for each time instant, and they are linked to each other by the common presence of the inverter / rectifier power flows:

$$\begin{cases} P_t^{PV}\hat{\eta}^{CHC} + P_t^{BESS\rightarrow}\hat{\eta}^{BESS\rightarrow} - \frac{P_t^{BESS\leftarrow}}{\hat{\eta}^{BESS\leftarrow}} - P_t^{inv} + P_t^{rect}\hat{\eta}^{rect} = 0 \\ P_t^{ICE} + P_t^{inv}\hat{\eta}^{inv} - P_t^{rect} = \frac{(\widehat{D}_t - \pi_t)}{\hat{\eta}^{distr}} \end{cases} \quad \forall t \qquad (1)$$

where:

- Power injected by the PV array on the DC bus is equal to the power produced by the panels (P_t^{PV}) multiplied by the efficiency of its power electronics ($\hat{\eta}^{CHC}$);
- Power injected by the battery on the DC bus is equal to the power discharging from the battery ($P_t^{BESS\rightarrow}$) multiplied by the battery discharging efficiency ($\hat{\eta}^{BESS\rightarrow}$);
- Power withdrawn from the DC bus by the battery is equal to the power charging the battery ($P_t^{BESS\leftarrow}$) divided by the battery charging efficiency ($\hat{\eta}^{BESS\leftarrow}$);
- P_t^{rect} is the power withdrawn from the AC bus and injected by the rectifier (with efficiency $\hat{\eta}^{rect}$) on the DC bus;
- P_t^{inv} is the power withdrawn from the DC bus and injected by the inverter (with efficiency $\hat{\eta}^{inv}$) on the AC bus;
- P_t^{ICE} is the power produced by the diesel ICE;
- $\frac{(\widehat{D}_t - \pi_t)}{\hat{\eta}^{distr}}$ is the power distributed from the AC bus to the final users: $\widehat{D}_t$ is the aggregate energy demand from the microgrid customers, π_t is the fraction of Non-Served Load, and $\hat{\eta}^{distr}$ is the efficiency of the distribution network.

Microgrid components are selected from an equipment catalog, where the technical and economical characteristics of different type of components are listed. Several PV and battery technologies are included in the catalog, each characterized by different values for a standard set of parameters. As for the ICEs, the catalog lists various models of different rated power that are available in the market. Table 3 lists the information about each component included in the database, while the details of the adopted numerical values are reported in appendix A. An exhaustive evaluation of the performance of the algorithm would require the examination of different equipment catalogs.

Unit	Technical parameters	Cost parameters
ICE	• Rated power • Load-fuel curve Min. load • Lifetime operating hours, • Start-up penalty	Machine cost Installment cost Yearly O&M
BESS	• Capacity • SOC limits • Charge/discharge η • Max ch./disch. Current • Nominal voltage • Battery model parameters • Lifetime energy throughput	Module cost Installment cost Yearly O&M
PV	• Rated power • Lifetime • Per unit hourly production profile as function of ambient temperature and solar irradiation	Module cost Installment cost Yearly O&M
INV/ REC	• Inverter efficiency • Rectifier efficiency • Inv/rect size ratio • Lifetime	Specific cost curve Installment cost Yearly O&M

Table 3: list of the characteristics of each component included in the database

Photovoltaic (PV) array

The PV array is constituted of a discrete number of modules, which determine the field nominal power. PV power production is obtained by multiplying the capacity installed by a nominal unitary production profile, representative of a typical yearly irradiance profile for the geographical location. Solar power production can be curtailed by acting on the PV charge controller, delivering only a fraction of the potential PV panel production on the DC bus. The maximum power exchanged with the DC bus determines the size of the PV charge controller, and therefore its cost. The efficiency of the charge controller is not dependent on its size.

Battery Energy Storage System (BESS)

The battery stack is constituted of a discrete number of modules, each with a nominal energy capacity and cost. A "two-tank" model is adopted for the battery, as described in [24]. The model is based on a linearization of the internal battery kinetic, and it divides the stored energy in two fractions, one readily available to be exchanged, and one chemically bonded within the battery and therefore not accessible to be exchanged at a given time. A set of equations describes the dynamic transition of energy from the bounded to the readily available state, as a function of the battery status and of its interactions with the DC bus. The equations include two experimental parameters, which allow for a tuning of the kinetic model, originally developed for lead acid batteries, to different battery technologies. Specifically, by setting high kinetic constants the entire energy content of the battery is collapsed in readily available energy, tracing back to a "single tank" model which is suitable for lithium ion batteries. A set of additional parameters specifies more information on the physical characterization of the battery, such as charge and discharge efficiency, rated voltage and current, and limitations in the depth of discharge. Each battery module is also characterized by a lifetime energy throughput, which represents the maximum energy flow that the module can sustain before having to be replaced. The actual lifetime of the battery is therefore a consequence of its size and of its yearly dispatch profile.

Inverter / Rectifier

The inverter is only needed if either a battery stack and/or a PV array is considered. Its size is determined by the maximum power exchange between the DC and AC buses. A fixed nominal power ratio is set between the inverter

and the rectifier modes, and the most restrictive condition deriving from the two opposite foreseen power flows sets its size. The inverter / rectifier efficiencies and lifetime are assumed to be independent from its size. A non-linear specific cost curve is obtained by interpolating a discrete dataset of commercial models, to take into account economies of scale.

Internal Combustion Engine (ICE)

A discrete list of ICEs is provided in the generation catalog. Each ICE is defined by a set of operating points, linking power production and fuel consumption as a function of the load level. In addition, maximum and minimum limits on the instantaneous power production are provided, as well as purchase and installment costs, yearly maintenance cost, and lifetime in terms of hours of operation. Actual lifetime is therefore a function of its yearly dispatch profile. A start-up penalty is also defined for each ICE model, representing the additional fuel consumption when the ICE is switched from off to on state. A continuous function of fuel consumption versus power production is constructed for each ICE from the set of operating points.

4. Microgrid generation and storage optimization

This section is focused on the description of the heuristic and predictive algorithms which, given a certain aggregate load profile, define the optimal configuration of generation and storage that minimizes the system annuitized total cost.

The design process is based on a two-step approach. First, the "*design sub-problem*" selects the optimal generation and storage configuration and size considering four weeks representative of the whole year. This choice is motivated by the need to limit the computational time and because usually only average seasonal data are available for any location. If the location shows a significant seasonal variation in radiation and/or demand patterns, typical weeks and their corresponding weights on the objective function would need to be determined by a more accurate clustering process, similarly to what is done in [25]. In this specific case, the low seasonality of the demand profiles within the region simplifies the selection process of the characteristic weeks, which have therefore been equally spaced in the year to cover the four seasons. An exhaustive evaluation of the algorithm would require the examination of different weather patterns. Second, the "*operation sub-problem*" tests the selected design over 8760 hours, providing the expected yearly operational cost for the system. The information obtained from both sub-problems are finally combined to provide a reliable LCOE estimate.

The two alternative methods that we shall examine here to determine the optimal design dispatch solution are the heuristic optimization algorithm (HA) and the predictive optimization algorithm (PA).

The HA relies on an iterative search in the design space, evaluating the performance of each candidate system configuration. Both in the "*design"* and "*operation"* sub-problems the heuristic and non-predictive Advanced Battery Valuation strategy [15] is adopted for dispatch decisions.

On the contrary, the PA solves the "*design sub-problem*" optimizing at the same time design and dispatch. The optimization problem is formulated as a single MILP: binary investment variables and machines operating set-points in all time instants constitute the variables of the optimization problem. The problem encompasses the entire design reference period, and therefore the optimization algorithm has a full knowledge of the future profiles of solar radiation. This approach has the advantage of being able to include system performance constraints over specific time spans, like a minimum annual system reliability or daily/weekly fuel consumption limits. However, the dispatch profile on which the PA bases its design is obtained from an unrealistic perfect knowledge of load and radiation profiles across the whole design reference period, which will result in somewhat optimistic operational costs. This assumption is smoothed by the adoption of reserve constraints which require upwards generation margins to be instantaneously available at all times. The final yearly performance evaluation removes this assumption, by solving a realistic "*operation sub-problem"*. This problem is solved adopting a rolling horizon (RH) approach, that ensures that the actual hourly dispatch strategy is optimized only based on near future (24 hours) information on RES energy production and load consumption, available with good confidence. The algorithm assumes perfect forecast for the next 24 hours. YALMIP [26] has been used to formulate the MILP in MATLAB,

A scheme of the main differences among the two methods and the two sub-problems is reported in Table 4

		HA	PA
Design sub-problem	**Output**	Optimal equipment sizing	Optimal equipment sizing
	Considered period	Four representative weeks	Four representative weeks

	Equipment typology and size	Optimized	Optimized
	Method of optimization	Grid search	MILP (“*one shot*”)
	Objective function	Minimization of system annuity	Minimization of system annuity
	Dispatch strategy	Pre-determined prioritization rules among resources, applied to actual operating conditions	Optimized
	Additional notes	Dispatch decision rules are independent from design decisions	Accurate BESS and ICE wear cost are included in the optimization and power reserve is enforced
	Output	Investment decisions	Investment decisions
Operation sub problem	**Considered period**	Full year (8760 hours)	Full year (8760 hours)
	Equipment typology and size	Fixed by the design sub-problem	Fixed by the design sub-problem
	Method of optimization	Rule based, applied to actual operating conditions	MILP (*Rolling Horizon*)
	Objective function	None. Rule based.	Minimization of operational cost, including BESS and ICE wear cost
	Dispatch strategy	Pre-determined prioritization rules among resources, applied to actual operating conditions	Optimized
	Additional notes	none	Power reserve is enforced
	Output	Yearly dispatch profiles	Yearly dispatch profiles, now with updated dispatch assuming perfect 24 hour forecast

Table 4: general scheme of the main differences between HA and PA approaches in the solution of design and operation sub-problems

The minimization of *system annuity* is the objective function for the selection of equipment sizing in both HA and PA “*design sub-problem*”. The system annuity represents the equivalent amount of money that an investor would have to spend each year to purchase, operate and maintain the microgrid for an indefinite amount of time and it can be calculated with the following equation:

$$system\ annuity = \sum_{j \in \left(\substack{components \\ installed}\right)} OPEX^{(j)} + \sum_{t \in \left(\substack{hours\ in \\ design \\ period}\right)} \frac{\left(C_{(t)}^{Fuel} + C_{(t)}^{Load.Shedding}\right)}{\chi_{RP}} + \sum_{i \in \left(\substack{components \\ installed}\right)} \frac{CAPEX^{(i)}}{AF^{(i)}} \quad (2)$$

Where:

- $C_{(t)}^{Fuel}$ is the hourly diesel consumption cost (diesel cost is assumed to be 1 $/l);
- $C_{(t)}^{Load.Shedding}$ represents a virtual non-served energy cost that accounts for the loss of utility due to electricity curtailments in the optimization routine;
- $OPEX^{(j)}$ is the yearly O&M for component j;
- χ_{RP} is the duration as fraction of a year of the design sub-problem reference period
- $CAPEX^{(i)}$ is the overall installation/replacement cost, which is sustained when the component is firstly purchased and every time it needs to be replaced;
- $AF^{(i)}$ is the annuity factor defined as a function of component lifetime ($LT^{(i)}$) and discount rate (dr):

$$AF^{(i)} = \frac{1 - (1 + dr)^{-LT^{(i)}}}{dr} \quad (3)$$

For some components like the PV panels or the inverter, the lifetime is fixed, while for others, as the ICE and the BESS, lifetime depends on their design and on the actual component usage pattern, that affects the wearing processes. For the ICE, a maximum number of operating hours during its lifetime has been considered ($\hat{H}_o^{ICE,MAX\ LT}$), while the lifetime of the BESS system is a function of the number of modules (n^{BESS}), the maximum energy throughput that can be provided by a single module during its lifetime ($\hat{E}^{BESS,MAX\ LT}$) and the actual yearly energy output ($E^{BESS,year}$). Lifetime for these components can be calculated with the following equations:

$$LT^{ICE} = \frac{\hat{H}_o^{ICE,MAX\ LT}}{H_o^{ICE,year}} \quad (4)$$

$$LT^{BESS} = \frac{n^{BESS}\hat{E}^{BESS,MAX\ LT}}{E^{BESS,year}} \quad (5)$$

It is worth noting that this link between dispatch strategy and component lifetime is fully accounted for by the PA method in the "*design sub-problem",* while for the HA approach it simply affects the *system annuity* calculation but not the dispatch strategy.

The LCOE is finally calculated as the ratio between the equivalent annual cost and the overall demand served. The equivalent annual cost for the system is calculated as the sum of:

- The annual equivalent investment cost for the selected equipment, as determined by the "*design sub-problem*" but updating the annuity factor of ICE and BESS based on their actual yearly usage determined by the "*operation sub-problem*"
- The annual operating cost associated to the dispatch profiles yielded by the solution of the "*operation sub-problem".* Load shedding cost is not included, since its scope is simply to affect the objective function, ensuring a higher quality of the service, but it does not represent a real cash flow.

4.1 Heuristic design algorithm (HA)[3]

The HA design approach is based on an exploration of the design space through a direct search method [27] that considers the system annuity as the function to be minimized. System annuity is calculated, for a given design configuration, by simulating system operation through the reference design period by adopting a heuristic dispatch strategy.
The heuristic dispatch strategy adopted follows, time step after time step, a prioritization among the available generation units, to cover for the instantaneous load and to charge the battery when convenient. No information about the future is exploited and the power reserve is implicitly accounted for in the dispatch priority rule. The dispatch prioritization list is built considering a specific energy production cost for each source: PV panels have null generation cost, ICEs generation cost is related to their efficiency, whereas the cost of load shedding (which can be considered as an equivalent load generation) must be selected according to the required reliability of the system [15]. The cost of using the battery as a generation unit is weighted relatively to the other generators proportionally to its present state of charge: the closer the battery is to its maximum SOC, the higher its ranking in the prioritization list will be.
The units are dispatched from the least costly up, saturating their generation capacity until the load is satisfied. The effectiveness of the dispatch method versus other well-known heuristic dispatch strategies (Cycle Charge, Load Following) is explored in [15].

The HA looks for an optimal microgrid design by exploring a search space of different combinations of sizes for PV, BESS and ICE. To enhance convergence and to avoid local minima, a bi-dimensional search for BESS and PV sizes is performed, fixing the ICE size. Starting from a center design point (red dot in Figure 4-left) the algorithm solves the hourly dispatch problem over the design sub-period for 8 surrounding combinations of PV and BESS sizes (blue points). In the following iteration, the center design point is moved to the point with the lowest system annuity among the ones explored thus far. If the new center is different from the previous one, the search radius identifying the neighbors remains unchanged (Figure 4-center) otherwise it is reduced (Figure 4-right). The search continues until the search radius is equal to the grid discretization.
An optimal combination of PV field and BESS sizes is identified for each ICE size considered. The ICE size is in turn varied according to two strategies: starting from the lowest to the highest reasonable ICE size available (the minimum size that can meet peak demand), and from the highest to the lowest. The two strategies stop the search when an annuity minimum with respect to ICE size is found (i.e. the annuity corresponding to optimal PV and BESS sizes increases with respect to the previous ICE size considered). The optimal solutions of the two strategies are then compared, and the one yielding the lowest annuity is selected as optimal design configuration.
Finally, the actual optimal system annuity is recomputed spanning the operation throughout the full characteristic year in the *operation sub-problem*.

[3] The heuristic algorithm employed in this paper is the one being used for microgrid optimization in a preliminary and simplified version of the Reference Electrification Model developed by the MIT/Comillas Universal Energy Access Lab. For more information see http://universalaccess.mit.edu.

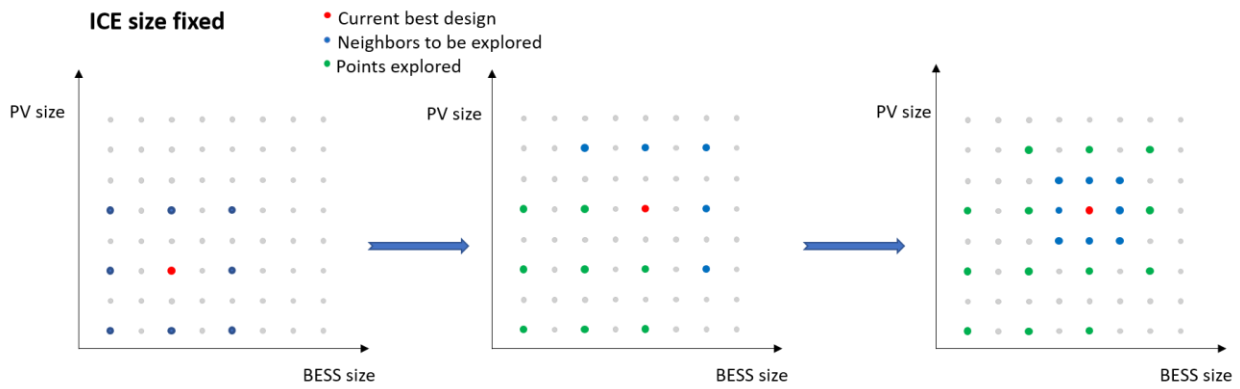

Figure 4: search algorithm for heuristic design

4.2 Predictive design algorithm (PA)

Differently from HA, the PA method is based for both the "*design"* and "*operation sub-problems"* on a Mixed Integer Linear Program (MILP) that can be written in the most general form as:

$$\min_{x} \boldsymbol{c}^T \boldsymbol{x}$$
$$s.t. \quad A\boldsymbol{x} \leq \boldsymbol{b} \tag{6}$$

Where $\boldsymbol{x}$ is the vector of variables, which includes: (i) investment decisions defining the microgrid design (namely typology and size of the installed equipment); (ii) dispatch variables that define the selected machines operation (set points, on / off state). The constraints include the energy balance equations on the microgrid for each time step, the operating limits and performance of the different components and, also, general constraints on the full period like fuel consumption limits or system reliability. The complete MILP formulation of the "*design sub-problem"* is provided in Appendix B.

Both the objective function and the constraints must be linear functions of the variables. The monotonically decreasing (in per unit) series of costs for inverters and PV power electronics, which exhibit an economy of scale with size, were substituted with a linear interpolation function, that fits the original curve in the surroundings of the expected equipment size. As for the power/fuel consumption curve of the ICEs, a single linear interpolation function was defined for the entire operating range, since the original curve is only mildly nonlinear.

In the objective function, the actualization coefficients for ICE and BESS investment cost are a non-linear function of both the investment and operation variables (eq. (4)-(5)). The actualized non-linear investment cost function is on the other hand convex with respect to its variables in the space of interest. It can therefore be approximated by means of a real variable, lower bounded by a family of linear constraints constituted by a set of lines (or planes) tangent to the original non-linear cost curve (or surface). In the optimal solution of the MILP, the annuitized cost linear proxy will be as low as possible, and therefore bounded by this set of constraints. The spacing of the tangent points determines the accuracy of the annuitized investment cost proxy and can be controlled arbitrarily by increasing the number of tangent points as shown in Figure 5.

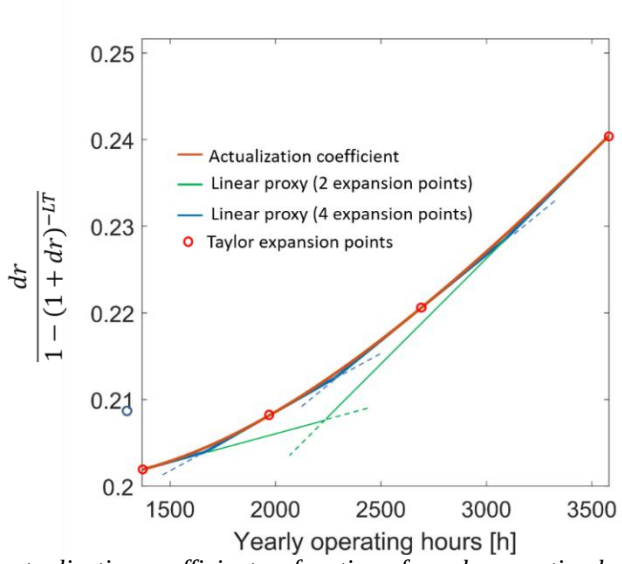

Figure 5 –Non-linear ICE actualization coefficient as function of yearly operating hours (orange line) and family of linear coefficients that serve as lower bound with adjustable precision. The linear proxy characterized by 4 expansion points follows more closely the actual value of the actualization coefficient.

A power reserve constraint is enforced both in the design and operation subproblems, to ensure that the system is able to face instantaneous and unforeseen variations of demand and PV production during real operation: in both subproblems a "spinning reserve" must be available at any time to face a simultaneous increase in demand and decrease in PV production. It is assumed that granted this margin, the ICE and BESS are capable to handle real-time active net demand variations and frequency regulation according to their droop curve and to a real-time redispatch algorithm. The maximum power contribution in each hour from BESS and ICE (if turned on) must therefore be able to potentially cover the worst-case net demand:

$$\hat{P}^{ICE,MAX} Z_{(t)}^{ICE} + \min\left(P_{(t)}^{BESS\rightarrow,MAX}, \frac{E_{(t)}^{BESS} - \hat{E}^{BESS,MIN}}{\widehat{\Delta t}}\right)\hat{\eta}^{BESS\rightarrow}\hat{\eta}^{inv} \qquad \forall t$$
$$\geq \left(1 + \widehat{\Delta D}^{\%}\right)\left(\hat{D}_{(t)} - \pi_{(t)}\right) - P_{(t)}^{PV}\left(1 - \widehat{\Delta PV}^{\%}\right)\hat{\eta}^{CHC}\hat{\eta}^{inv} \qquad (7)$$

Where:

- $\hat{P}^{ICE,MAX}$ is the maximum power that can be provided by the ICE;
- $Z_{(t)}^{ICE}$ is the binary variable that defines if the ICE is switched on (1) or off (0);
- $P_{(t)}^{BESS\rightarrow,MAX}$ is the maximum power that can be provided by the battery stack;
- $E_{(t)}^{BESS}$ is the energy content of the battery at time *t*;
- $\hat{E}^{BESS,MIN}$ is the minimum energy content of the battery to avoid excessive wear related to deep discharge;
- $\widehat{\Delta D}^{\%}$ and $\widehat{\Delta PV}^{\%}$ are the percentage variations to be considered for energy demand and PV production respectively, in defining the worst-case net power that serves as spinning reserve requirement. Both are set to 25%. The effect of reserve margins on real operation operating cost has been explored in [17], quantifying their effect on the real system operation cost as a function of the forecast accuracy.

Since the dispatch strategy in the "*design sub-problem"* can benefit from the unrealistic exact knowledge of future PV and load trends, the actual yearly operation cost is computed, after fixing the design, in the "*operation sub-problem*" with a more realistic *rolling horizon* (RH) methodology: the dispatch MILP is conservatively solved for a limited future horizon (24 h), for which weather and demand forecasts are known with perfect accuracy. Once the problem is solved, the obtained solution is implemented only for an initial fraction of the time (6 h), then the starting time is moved forward, and the procedure is repeated until the entire time range has been spanned. It is

acknowledged that the perfect 24 hour forecast provides some advantage over the actual operation over an uncertain horizon, but we are relying of the good quality of 24 hour ahead forecasts and on its update every 6 hours.
The objective function of each dispatch MILP is the minimization of the operational cost of the system. To account for the wear cost of BESS and ICE an average wear cost is included in the dispatch MILP objective function as reported in equation (8). This formulation of the wear cost leads the yearly operation dispatch to converge to a value of BESS and ICE lifetime close to what is found as optimal in the "*design sub-problem"*, tuning the actualized investment cost achieved by the two simulations.

$$C_{wear(j)} = \frac{Annuity_{design\,(j)}}{Yearly\ Usage_{design\,(j)}}(RH\ Usage_{(j)}) \quad j \in \{BESS, ICE\} \tag{8}$$

The final system annuity is computed based on the optimal microgrid configuration (determined by the *design sub-problem*) and the optimal dispatch strategy (determined by the *operation sub-problem*). All relevant non-linear cost functions are included in their non-linear form in this last stage. Therefore, all errors introduced by the MILP linearization process can only influence the quality of the optimal MILP solution, not the value of the LCOE itself.

4.3 Comparison of HA and PA design and operation

The microgrid design and operation have been optimized with the two design algorithms for a diverse set of users of increasing size, although an exhaustive comparison over different equipment catalogs and weather patterns is pending. Maintaining on average the same region-wide proportion between users of different classes, multiple aggregate load profiles were created, varying the total number of users, users' type mix, and random association of each user to a characteristic profile from the profile library, to assess the differences between PA and HA approaches over a wide range of cases. Random processes are harmonized when comparing solutions obtained from the PA and the HA by means of a common random seed. Microgrid sizes go from stand-alone systems including only one building to a large unique system encompassing the whole region.
Table 5 shows a comparison between PA and HA optimal component sizing for the 10 synthetic microgrids whereas Figure 6 shows the percentage savings achieved by the PA for all the investigated microgrids.
For microgrids with low annual energy demand no ICE is installed, since the high specific cost of small size ICEs and their low generation efficiency make them not competitive with purely solar electricity generation plus storage. For PV-BESS only systems the annuity reduction attained with PA is between 2% and 4%, due to the relatively straightforward identification of an optimal dispatch strategy for non-complex systems. A transition zone can be observed for annual energy demand of about 75-100 MWh/year, where the architecture of the optimum design that is obtained by the two methods is different. Here, the PA includes an ICE in the system as opposed to a costlier PV-BESS system designed by the heuristic method. As the installation of an ICE becomes feasible, the advantage attained by the PA sharply increases to 6-9%, denoting the better ability of the proposed routine to manage the operational degree of freedom given by the engine, and of exploiting it in conjunction with the buffer capacity of the battery to optimize the ICE fuel consumption and battery wear (we acknowledge the advantage provided by the 24 hour perfect forecast). Finally, at even higher sizes both methods feature an ICE, but the PA consistently opts for a larger PV array, and manages to minimize PV curtailment and to optimize the usage of the smaller ICE by exploiting the flexibility granted by the adoption of a very large BESS.

			HEURISTIC OPTIMA							**PREDICTIVE OPTIMA**						
Users	**Yearly Energy kWh**	**Peak Power kW**	**BESS kWh**	**PV kW**	**ICE kW**	**CAPEX $**	**OPEX $**	**Annuity $**	**LCOE $/kWh**	**BESS kWh**	**PV kW**	**ICE kW**	**CAPEX $**	**OPEX $**	**Annuity $**	**LCOE $/kWh**
1	157.5	0.09	0.65	0.14	0	115.67	71.95	195.4	1.253	0.57	0.14	0	111.05	71.71	191.0	1.225
4	1027	0.65	4.18	1	0	451.36	85.94	558.3	0.534	3.94	1	0	435.68	84.81	543.8	0.518
12	3041	1.59	10.75	2.75	0	1124.6	112.8	1342	0.421	10.47	3	0	1139.3	112.4	1295	0.418
34	8245	5.04	32.9	8	0	3330.7	195.1	3686	0.436	30.9	7.75	0	3228.3	187.5	3607	0.424
101	24630	14.7	99.8	23	0	9576	436.4	10630	0.417	93.1	22.5	0	9285.5	413.3	10379	0.405
301	75150	44.1	291	70	0	28654	1163	31735	0.407	121	34.25	40	14716	14812	29550	0.393
894	2.31e5	131.3	127.6	62	100	26018	57396	85735	0.365	248.5	84.25	100	32526	46307	78996	0.342

2664	6.85e5	390.7	378.5	180	300	77145	1.62e5	2.45e5	0.353	692.1	231.8	300	91565	1.36e5	2.28e5	0.333
7940	2.08e6	1167	861.9	614	1000	2.22e5	4.93e5	7.26e5	0.346	2266	756.3	750	2.96e5	3.87e5	6.83e5	0.329
40810	1.07e7	6000	2950	3143	6000	1.06e6	2.65e6	3.74e6	0.348	10320	3607	4000	1.40e6	2.09e6	3.49e6	0.327

Table 5: optimal heuristic and predictive microgrid design for different microgrid sizes

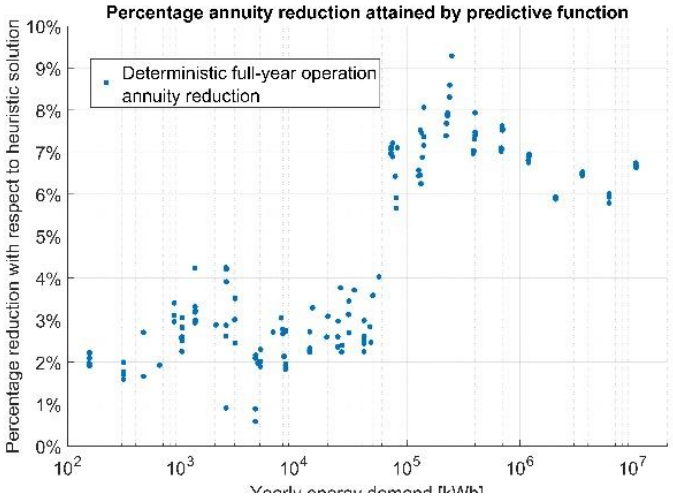

Figure 6: annuity reduction by adopting the predictive design algorithm for various microgrids

Figure 7 shows the LCOE trend and break-up as a function of microgrid size, for the HA and PA approaches (left and right stacks respectively). Economies of scale make larger microgrids cheaper per unit output. On the other hand, connecting users in areas with low density of demand will imply larger distribution networks with higher connection costs. BESS is the main cost for stand-alone and small microgrids while fuel is the major cost index for systems featuring an ICE. Therefore, an optimal dispatch of the engine is a key factor in reducing the total cost of microgrid design, explaining the increase in energy cost relative difference between HA and PA for large systems.

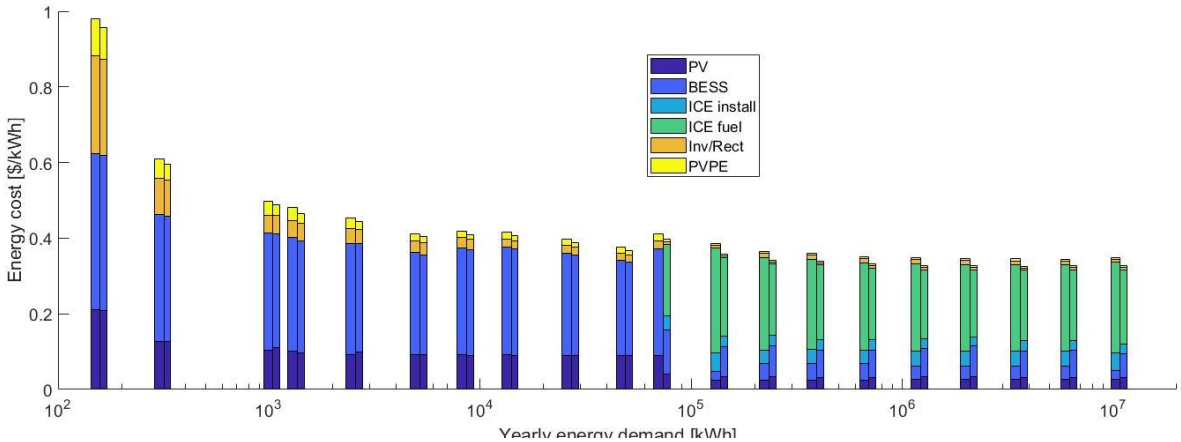

Figure 7: LCOE break-up for microgrid of increasing size, for heuristic (left bar) and predictive (right bar) optimal design

The optimal management of the ICE results in a higher percentage of production from renewable resources for large systems, consistently achieving a percentage of overall energy production from PV which is about 10 percentage points higher for the PA as reported in Figure 8-left. Finally, the predictive approach also results in higher average system reliability for small microgrids supplied by just PV and BESS and reaching a nearly 0% load shedding once an ICE is installed as reported in Figure 8-right. This reflects in an annuity reduction attained by the PA over the

HA, which is generally greater than the corresponding LCOE reduction since, differently from the LCOE, the annuity explicitly accounts for the non-served energy penalty. Including the integrated production planning of additional energy-related goods in addition to electricity, as proposed by the authors in [28], would increase the degrees of freedom exploitable by MILP optimization, and lead to even further energy cost reduction.

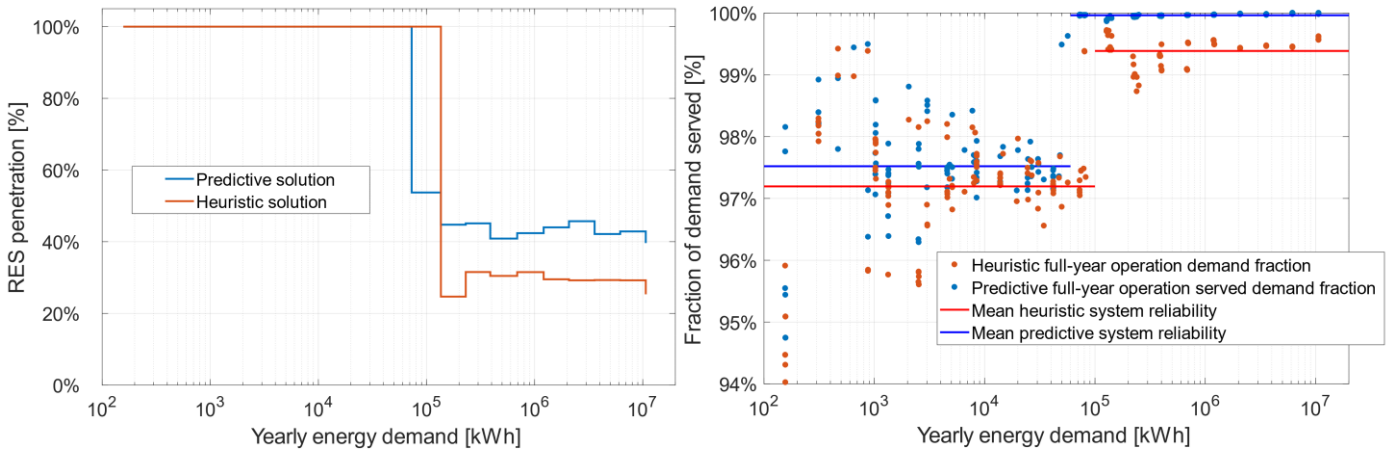

Figure 8: (left) renewable share of energy generation for microgrids of various sizes, (right) fraction of demand served in heuristic (red) and predictive (blue) optimal designs, for various microgrid sizes

5. Application to regional electrification planning

5.1 Regional electrification planning method

The differences in microgrid design and performance between the HA and PA approaches are also expected to lead to different results when the two algorithms are used in an electrification planning model for a region, where the three electrification modes – grid extension, microgrids and stand-alone systems – compete with one another.

Figure 9 shows the structure of the master algorithm adopted to solve the regional electrification problem. A preliminary and simplified version of the Reference Electrification Model (REM) developed by the MIT/Comillas Universal Energy Access Lab has been used for this purpose [29]. Input to the algorithm is a full description of the nature of the problem, and of the resources available to address it: (i) layout, rating and reliability performance of existing electric grid lines, that can serve as starting point to branch off new lines that electrify new groups of on-grid users; (ii) location and latent energy usage pattern of non-electrified users; (iii) technical and economical characterization of the generation and storage equipment that can be employed in the design of microgrids (please refer to appendix A for further details) (iv) terrain topography and local solar availability in the form of hourly radiation profile for a typical year; (v) technical and economical characterization of all equipment for MV and LV distribution networks.

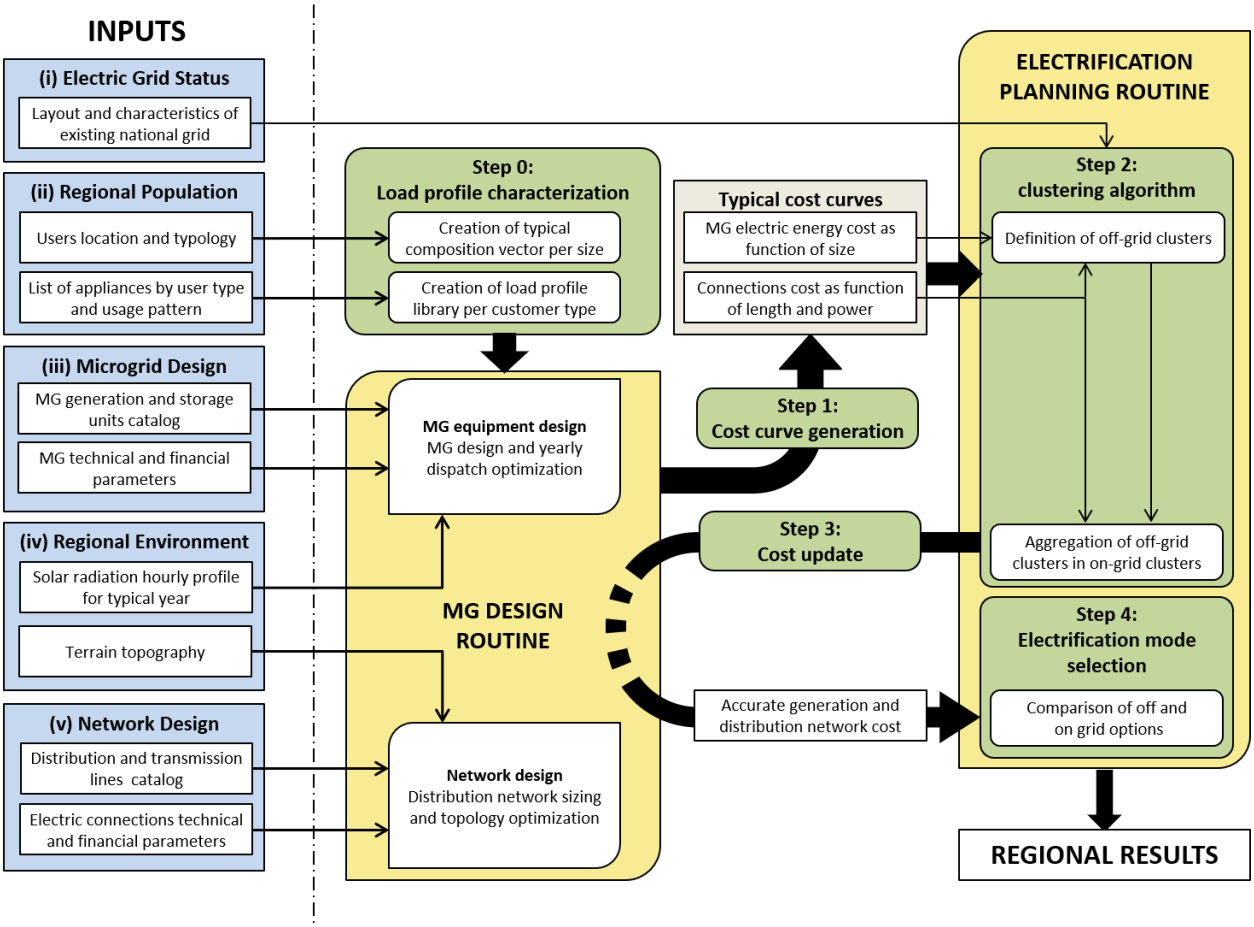

Figure 9: regional electrification algorithm

The algorithm is based on the interaction of two main routines:

- The first routine (*MG Design*) optimizes the design of the generation and storage systems and of the distribution network for a local microgrid electrifying a given group of users. The optimization of the microgrid equipment is performed by either the PA or the HA. The design of the distribution network, including layout and sizing of all necessary equipment, is performed using the well-proven Reference Network Model (RNM), which explicitly accounts for the potential presence of topography and distributed power injection points in designing the network [30].
- The second routine (*Electrification planning*) begins by defining the optimal aggregation of users in clusters, for which the *on-* and *off-grid* electrification options are compared. Clusters are defined by the progressive aggregation of users, driven by the trade-off between lowering the resulting LCOE versus increasing the cost of connecting all microgrid users.

Ideally, the selection of the optimal customer clustering should be performed simultaneously to the design of the electrification infrastructures and the equipment selection for each microgrid. However, the highly interconnected nature of the problem would lead to unfeasible computational efforts to reach the final solution. To simplify the problem, the clustering algorithm at the core of the *Electrification planning* routine takes its decisions based on cost curves for both electricity production and distribution network, generated a priori by the *MG Design* routine considering reference cases of the different sizes characterizing the composition of the region.

Following the clustering step, detailed electrification projects for the SA, MG, and GE options are designed, and the one with lowest net present cost over a certain planning horizon is chosen on each case.

5.2 Regional Electrification planning results

The general methodology outlined was applied to determine the optimal electrification plan for the test case region. First, a reference scenario was obtained by forcing the regional planning model to consider only the grid-extension option with a flat price of the wholesale energy provided to the MV grid of 20 c$/kWh. The resulting total average cost for the end user (which includes the actualized investment cost for all new infrastructures) is about 60 c$/kWh. Grid reliability is assumed to be 99%.

Second, the analysis has been carried out including electrification via off-grid systems (microgrids and stand-alone buildings), either resorting to the HA or the PA for design and dispatch definition.

Figure 10 shows the number of microgrids included in the optimal regional solution versus the aggregated annual demand in the region, when either the HA or the PA is adopted. The monotonically decreasing value of LCOE as a function of system size (which is obtained by fitting a large set of optimal results such as those reported in Figure 8) is the main driver of the clustering process. The number of microgrids in the final solution, as well as the overall energy production share from off-grid systems, are substantially increased when the PA is adopted, as a result of the lower energy cost attained with this approach. The average microgrid size is larger in the PA solution, reflecting the higher economical advantage for systems large enough to adopt an ICE and that can effectively benefit from the adoption of a predictive approach. The differences in share of on- versus off-grid users to which the two solution instances converge are qualitatively shown in Figure 11, where the location of each user is highlighted in different colors according to the optimal electrification mode identified. The reduction in energy cost for microgrid users attained by the PA makes microgrids more competitive as an alternative to grid extension in electrifying users. As a result, the predictive regional solution opts for an electrification plan dominated by microgrids in large geographical areas that the heuristic solution has mostly assigned to grid extension.

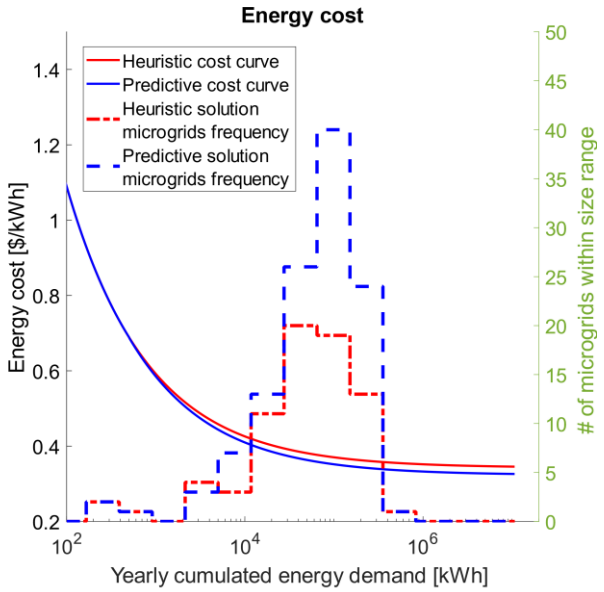

Figure 10: reference LCOE curves and frequency histograms of various sizes off-grid microgrid in the optimal regional solution

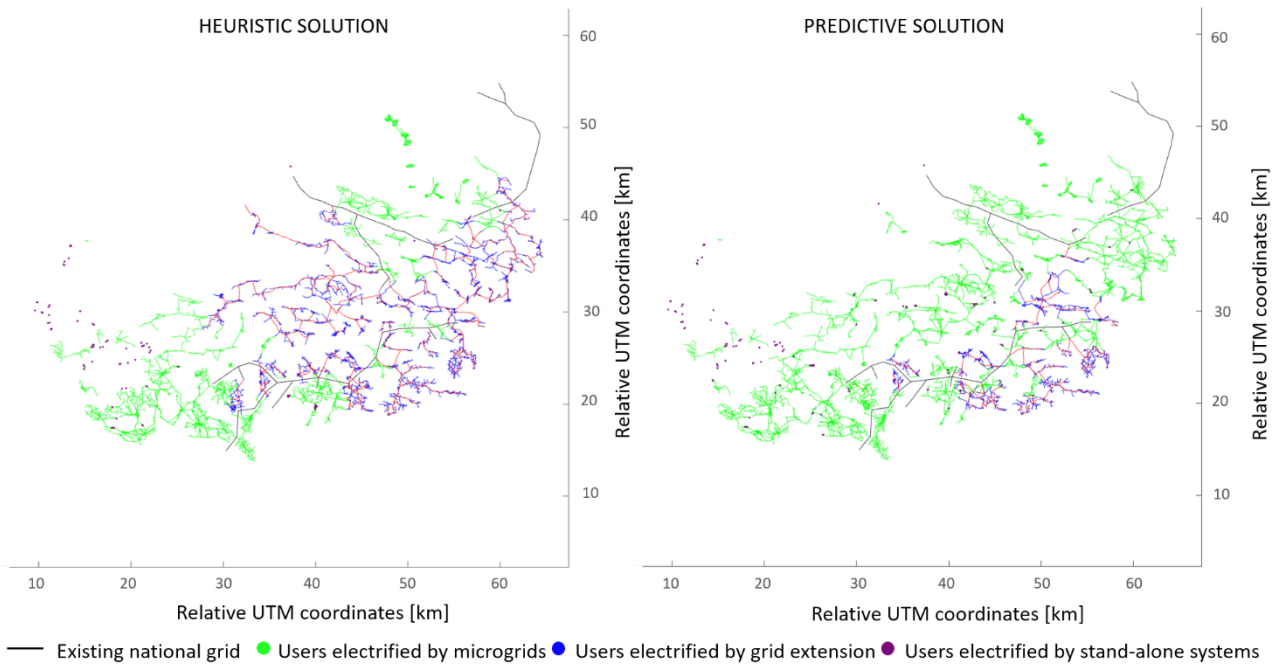

Figure 11: layout of optimal regional solution, when adopting the heuristic (left) or the predictive (right) microgrid design routine

Table 6 depicts the main results for the optimal electrification plan obtained with the predictive and the heuristic solutions, showing that the use of the PA method allows (i) to strongly increase the number of customers served by microgrids and stand-alone systems compared to grid connected ones and (ii) to reduce the LCOE as compared to both HA and to the reference scenario case where only grid extension is considered. The optimal economic results of the two instances are on the other hand very similar, with a reduction of the regional annuity in the predictive solution which is below 1% since the total energy cost of large microgrids (including network and new infrastructure) is similar for both PA and HA. A larger cost reduction would be attainable considering more complex multi-good systems where the use of PA approach can lead to larger advantages compared to HA. Finally, it is worth noting that sufficiently large microgrids can lead to a real electrification cost reduction, while at the same time providing a large share of energy from renewable sources, an increase system reliability, and a modular investment that could be promoted in close contact with local communities. Specifically, regional service reliability increases to 99.5% when microgrids are included and the PA is adopted while it remains 99% when resorting to the HA.
Two additional cases have been considered to illustrate the differences between the PA and HA approaches:

- If the flat price of the wholesale energy provided to the national grid is lower than the base case and equal to 15 c$/kWh the share of users served by the national grid is increased up to around 77% in both solutions. Resorting to the PA still leads to a lower average electricity cost with respect to the HA (-1.26%). Regional reliability is very similar in the two cases, being respectively 99% and 98.8% for the PA and the HA cases.
- On the contrary if the flat price of the wholesale energy provided by the national grid is equal to 25 c$/kWh, electrification by grid extension is abandoned by the PA solution, in which the totality of the users within the region is served by microgrids. The HA solution on the other hand still features a 20% share of customers connected to the grid. In this scenario, the advantage in using the PA approach is more marked, since the optimal solution moves toward larger microgrids for which the cost savings are larger respect to the HA method, resulting in a lower average electricity cost (-2.83%). Regional reliability is also significantly higher for the PA solution, being 99.5% versus 98.9% for the HA solution.

		PREDICTIVE SOLUTION				**HEURISTIC SOLUTION**			
National grid electricity flat price	**System Type**	microgrids	Stand alone	Grid connected	Total	microgrids	Stand alone	Grid connected	Total

20 c$/kWh	# of Customers	30991	153	9666	40810	17022	94	23694	40810
	LCOE ($/kWh)	0.564	0.89	0.549	0.558	0.577	0.87	0.557	0.566
15 c$/kWh	# of Customers	9911	61	30838	40810	8932	21	31857	40810
	LCOE ($/kWh)	0.551	0.78	0.516	0.524	0.560	0.75	0.523	0.532
25 c$/kWh	# of Customers	40638	172	0	40810	32601	124	8085	40810
	LCOE ($/kWh)	0.559	0.90	-	0.559	0.574	0.90	0.600	0.579

Table 6: regional economic results summary for three different flat prices of the wholesale energy from the national grid.

6. Conclusions

This paper compares two alternative approaches for the optimization of design and dispatch profiles of rural microgrids. The Predictive Algorithm (PA) is based on the solution of a Mixed Integer Linear Program, whereas the Heuristic Algorithm (HA) performs a search of the design space applying predefined dispatch rules. Both are applied to the local electrification of rural communities of a Sub-Saharan African region. The differences between the two optimization methods are examined both in the local design of individual microgrids as well as for regional electrification planning. For the latter, a case example using a regional planning model illustrates the potential impact of adopting different microgrid design approaches on the optimal electrification plan, both in cost and the mix of delivery modes.

As revealed by the local comparison, the main advantages of the PA with respect to HA are:

- In HA, the optimal design of PV and BESS results from a modified pattern search method that may incur in local minima, as well as with the search of the optimal ICE. Multiple launching of the optimization process or examination of all the possible combinations of PV, BESS and ICE generally results in an unacceptable computational time. The PA method modifies the problem formulation with a linear approximation that allows computing the microgrid optimal design and dispatch by solving a *one-shot* MILP problem.
- The HA dispatch strategy is based on a heuristic rule that allows to deal with each time step independently from the others and ignores the consequences of these hourly decisions on the overall yearly performance. As a result, HA cannot develop dispatch strategies that account for component wear or annual constraints, for instance. The only option for HA is to penalize a-posteriori the solutions that do not satisfy these global criteria, potentially discarding optimal design configurations that, with proper dispatch decisions, would be capable of respecting the constraint.
  On the contrary, the PA method considers component design and operation dispatch jointly, as well as the entire optimization horizon. This allows PA to include easily component wearing costs and general constraints like a minimum annual system reliability or maximum fuel consumption. An obvious drawback of PA is that it assumes a perfect knowledge of uncertain events over the period of optimization. However, a realistic performance of the design obtained with PA can be obtained by simulating its operation with a predictive MILP optimization algorithm. It remains for further research to take advantage of the "anticipative vision of the PA method" to design heuristic operation rules that mimic the optimal behavior observed in the solution given by PA.
- The numerous tests performed with both algorithms designing microgrids show that PA leads to a lower cost of electricity, a higher system reliability and a larger penetration of renewable energy for all the investigated cases. These advantages are more marked for more complex microgrid architectures that include an ICE in addition to PV and BESS, and in the presence of dispatchable loads or multi-commodity systems. In the context of electrification planning at regional scale, the PA method with respect to HA leads to plans characterized by a larger number of customers served by microgrids and standalone systems, as well as a lower average regional electricity cost.

Despite its advantages, two limitations of the PA approach have to be pointed out:

- The MILP formulation adopted in the PA method requires a linearization of all non-linear equations. Thus, MILP may fail the identification of the optimal design if the linearized functions differ from the original ones significantly. The error can be reduced by a better approximation of the nonlinear functions, but this results in an increase of the problem complexity and computational time. HA does not have any restriction on the model formulation.
- Ad hoc cost terms (e.g. appropriately tuned wear cost terms) must be included in the formulation of the dispatch MILP to enforce the consistency between "*design sub-problem"* and "*operation sub-problem*" calculations. Instead, HA solves both problems with the same operation rules, thus ensuring that the system is dispatched consistently with the criteria used in the design process.

7. Acknowledgments

This work was developed as part of the collaboration between MIT Energy Initiative and Politecnico di Milano Group of Energy COnversion Systems (GECOS), sponsored by the "Progetto Roberto Rocca". L. Moretti gratefully acknowledges the MIT/Comillas Universal Access Lab for their hospitality and support.

8. References

[1] UN, "Energy for a Sustainable Future. Report and Recommendations.," New York, 2010.

[2] S. C. Bhattacharyya, "Electrification Experiences from Sub-Saharan Africa," in *Rural electrification through decentralised off-grid systems in developing countries*, Springer, London, 2013, pp. 131–156.

[3] IRENA, "Renewable Power Generation Costs in 2017," *Int. Renew. Energy Agency*, 2018.

[4] S. Mandelli, J. Barbieri, R. Mereu, and E. Colombo, "Off-grid systems for rural electrification in developing countries: Definitions, classification and a comprehensive literature review," *Renew. Sustain. Energy Rev.*, vol. 58, pp. 1621–1646, May 2016.

[5] J. P. Murenzi and T. S. Ustun, "The case for microgrids in electrifying Sub-Saharan Africa," in *IREC2015 The Sixth International Renewable Energy Congress*, 2015, pp. 1–6.

[6] S. Szabó, K. Bódis, T. Huld, and M. Moner-Girona, "Energy solutions in rural Africa: mapping electrification costs of distributed solar and diesel generation versus grid extension Energy solutions in rural Africa: mapping electrification costs of distributed solar and diesel generation versus grid extensi," *Environ. Res. Lett. Environ. Res. Lett*, vol. 6, pp. 34002–9, 2011.

[7] K. Ubilla *et al.*, "Smart Microgrids as a Solution for Rural Electrification: Ensuring Long-Term Sustainability Through Cadastre and Business Models," *IEEE Trans. Sustain. Energy*, vol. 5, no. 4, pp. 1310–1318, Oct. 2014.

[8] P. Del Rıó and M. Burguillo, "Assessing the impact of renewable energy deployment on local sustainability: Towards a theoretical framework," *Renew. Sustain. Energy Rev.*, vol. 12, pp. 1325–1344, 2008.

[9] N. J. Williams, P. Jaramillo, J. Taneja, and T. S. Ustun, "Enabling private sector investment in microgrid-based rural electrification in developing countries: A review," *Renew. Sustain. Energy Rev.*, vol. 52, pp. 1268–1281, 2017.

[10] A. G. Dagnachew, P. L. Lucas, A. F. Hof, D. E. H. J. Gernaat, H.-S. de Boer, and D. P. van Vuuren, "The role of decentralized systems in providing universal electricity access in Sub-Saharan Africa – A model-based approach," *Energy*, vol. 139, pp. 184–195, Nov. 2017.

[11] F. F. Nerini, O. Broad, D. Mentis, M. Welsch, M. Bazilian, and M. Howells, "A cost comparison of technology approaches for improving access to electricity services," *Energy*, vol. 95, 2016.

[12] A. Chauhan and R. P. Saini, "A review on Integrated Renewable Energy System based power generation for stand-alone applications: Configurations, storage options, sizing methodologies and control," *Renew. Sustain. Energy Rev.*, vol. 38, pp. 99–120, 2014.

[13] M. Husein and I.-Y. Chung, "Optimal design and financial feasibility of a university campus microgrid considering renewable energy incentives," *Appl. Energy*, vol. 225, pp. 273–289, Sep. 2018.

[14] "HOMER - Hybrid Renewable and Distributed Generation System Design Software." [Online]. Available: https://www.homerenergy.com/. [Accessed: 31-Jul-2018].

[15] V. Li, "The Local Reference Electrification Model : comprehensive decision-making tool for the design of rural microgrids," Massachusetts Institute of Technology, Boston, 2016.

[16] S. Mazzola, M. Astolfi, and E. Macchi, “The potential role of solid biomass for rural electrification: A techno economic analysis for a hybrid microgrid in India,” *Appl. Energy*, vol. 169, pp. 370–383, 2016.
[17] S. Mazzola, C. Vergara, M. Astolfi, V. Li, I. Perez-Arriaga, and E. Macchi, “Assessing the value of forecast-based dispatch in the operation of off-grid rural microgrids,” *Renew. Energy*, vol. 108, pp. 116–125, Aug. 2017.
[18] Lawrence Berkeley National Laboratory, “Distributed Energy Resources - Customer Adoption Model (DER-CAM) | Building Microgrid.” [Online]. Available: https://building-microgrid.lbl.gov/projects/der-cam. [Accessed: 06-Aug-2018].
[19] L. Ferrer-Martí, B. Domenech, A. García-Villoria, and R. Pastor, “A MILP model to design hybrid wind-photovoltaic isolated rural electrification projects in developing countries,” *Eur. J. Oper. Res.*, vol. 226, pp. 293–300, 2013.
[20] E. D. Mehleri, H. Sarimveis, N. C. Markatos, and L. G. Papageorgiou, “Optimal design and operation of distributed energy systems: Application to Greek residential sector,” *Renew. Energy*, vol. 51, pp. 331–342, 2013.
[21] D. Ellman, “The Reference Electrification Model: A Computer Model for Planning Rural Electricity Access,” Massachusetts Institute of Technology, Boston, 2015.
[22] “Shuttle Radar Topography Mission.” [Online]. Available: https://www2.jpl.nasa.gov/srtm/. [Accessed: 12-Aug-2018].
[23] V. Salas, W. Suponthana, and R. A. Salas, “Overview of the off-grid photovoltaic diesel batteries systems with AC loads,” *Appl. Energy*, vol. 157, pp. 195–216, 2015.
[24] J. F. Manwell and G. Jon, “Lead acid battery storage model for hybrid energy systems,” *Sol. Energy*, vol. 50, no. 5, pp. 399–405, 1993.
[25] J. Sachs and O. Sawodny, “Multi-objective three stage design optimization for island microgrids,” *Appl. Energy*, vol. 165, pp. 789–800, Mar. 2016.
[26] J. Lofberg, “YALMIP : a toolbox for modeling and optimization in MATLAB,” *2004 IEEE Int. Conf. Comput. Aided Control Syst. Des.*, pp. 284–289, 2004.
[27] R. Hooke and T. A. Jeeves, “`` Direct Search’’ Solution of Numerical and Statistical Problems,” *J. ACM*, vol. 8, no. 2, pp. 212–229, Apr. 1961.
[28] M. Astolfi, S. Mazzola, P. Silva, and E. Macchi, “A synergic integration of desalination and solar energy systems in stand- alone microgrids,” *Desalination*, vol. 419, pp. 169–180, Oct. 2017.
[29] “Universal Access Lab - MIT & IIT-Comillas.” [Online]. Available: http://universalaccess.mit.edu/#/main. [Accessed: 13-Feb-2018].
[30] C. Mateo Domingo, T. Gomez San Roman, Á. Sanchez-Miralles, J. P. Peco Gonzalez, and A. Candela Martinez, “A Reference Network Model for Large-Scale Distribution Planning With Automatic Street Map Generation,” *IEEE Trans. Power Syst.*, vol. 26, no. 1, pp. 190–197, Feb. 2011.

APPENDIX A

ICE																	
Size (kW)	**1/4 Load (l/kWh)**	**1/2 Load (l/kWh)**	**3/4 Load (l/kWh)**	**Full Load (l/kWh)**	**Min power**	**Cost (USD)**	**O&M ($/y)**	**Startup fuel (l)**	**Size (kW)**	**1/4 Load (l/kWh)**	**1/2 Load (l/kWh)**	**3/4 Load (l/kWh)**	**Full Load (l/kWh)**	**Min power**	**Cost (USD)**	**O&M ($/y)**	**Startup fuel (l)**
5	0.500	0.442	0.408	0.385	0.5	3200	160	-	250	0.345	0.288	0.275	0.273	25	50000	2500	2.64
8	0.493	0.436	0.402	0.379	0.8	4119	206	-	300	0.343	0.285	0.271	0.271	30	60000	3000	3.40
10	0.489	0.432	0.398	0.376	1	4643	232	-	350	0.342	0.283	0.270	0.271	35	70000	3500	4.25
15	0.478	0.423	0.390	0.368	1.5	5773	289	-	400	0.337	0.282	0.269	0.272	40	80000	4000	5.17
20	0.468	0.414	0.381	0.360	2	6737	337	-	500	0.333	0.280	0.266	0.270	50	100000	5000	6.86
25	0.458	0.405	0.373	0.352	2.5	7595	380	-	600	0.333	0.278	0.265	0.270	60	120000	6000	8.72
30	0.448	0.397	0.366	0.345	3	8376	419	-	750	0.329	0.277	0.264	0.269	75	150000	7500	11.49
40	0.430	0.381	0.351	0.331	4	9776	489	-	1000	0.327	0.276	0.263	0.269	100	200000	10000	16.11
60	0.399	0.353	0.325	0.307	6	12154	608	-	1250	0.326	0.274	0.262	0.269	125	250000	12500	21.14
80	0.371	0.329	0.303	0.286	8	16080	709	-	1500	0.325	0.274	0.262	0.269	150	300000	15000	26.57
100	0.371	0.310	0.293	0.280	10	20000	1000	0.49	1750	0.324	0.273	0.262	0.269	175	350000	17500	32.41
125	0.370	0.303	0.287	0.276	12.5	25000	1250	0.71	2000	0.324	0.273	0.261	0.269	200	400000	20000	38.66
135	0.368	0.303	0.284	0.275	13.5	27000	1350	0.87	2250	0.324	0.273	0.261	0.268	225	450000	22500	45.31
150	0.363	0.298	0.283	0.275	15	30000	1500	1.10	3000	0.323	0.272	0.261	0.268	300	600000	30000	65.25
175	0.355	0.294	0.280	0.275	17.5	35000	1750	1.42	4000	0.321	0.270	0.261	0.268	400	800000	40000	91.85
200	0.356	0.291	0.278	0.273	20	40000	2000	1.78	6000	0.319	0.267	0.260	0.267	600	1200000	60000	145.04
230	0.349	0.290	0.274	0.273	23	46000	2300	2.24	8000	0.316	0.263	0.259	0.267	800	1600000	80000	198.23

Installation Costs as fraction of generator cost [-]	0.8	**Annual O&M as a fraction of generator cost**	0.05	**Lifetime [h]**	35000	**Annual O&M man-hours (mhrs)**	25

BESS														
Battery Technology	**Cost [$]**	**Installation Cost [$]**	**Annual O&M [$]**	**Annual O&M mhrs**	**Energy Capacity [kWh]**	**Min. SOC [-]**	**Max. SOC [-]**	**charge / discharge η [-]**	**Max charge current [A]**	**Max discharge current [A]**	**Nominal voltage [V]**	**Lifetime throughput [KWh]**	**KiBaM Parameters**	
													c [-]	**k [1/hr]**
Lithium Ion	14.4	2.9	0.14	5	0.07168	0.1	1	0.95	1.4	2.6	51.2	10.8	1	1
Lead Acid	150	30.0	1.50	5	1.38	0.3	1	0.922	11	NA	6	845	0.281	1.85

PV					
Panel Size (kW)	**Cost ($)**	**Lifetime [y]**	**Installation Costs [$]**	**Annual O&M [$]**	**Annual O&M mhrs**
0.25	125	25	50	1.25	5
0.02	12	25	2.4	0.12	5

INVERTER / RECTIFIER										
Models for cost curve construction	Costs ($/kW)	927	740	395	364	319	260	220	190	190
	Sizes (kW)	0.15	0.2	0.4	1	1.5	5	6	10	11.4
Installation Costs as fraction of converter cost		0.1		**Rectifier Efficiency**	0.9	**Annual O&M mhrs**	2		**Life (years)**	15
Annual O&M as a fraction of converter cost		0.01		**Inverter Efficiency**	0.95	**Rectifier / Inverter Capacity Ratio**	0.8		**Min Size (kW)**	0.15

PV CHARGE CONTROLLER							
Models for cost curve construction	Costs ($/kW)	481	375	283	215	133	131
	Sizes (kW)	0.054	0.12	0.24	1.44	3.84	4.128
Min Size (kW)	0.054	**Lifetime [y]**	15	**Efficiency**	0.95	**Annual O&M mhrs**	2
Installation Costs as fraction of charge controller cost			0.1	**Annual O&M as a fraction of charge controller cost**			0.01

APPENDIX B

SETS:

$T = \{1..n_t\}$: set of timesteps

$COMP = \{ICE, BESS, PV, CHC, IR\}$: set of all microgrids components, including Internal Combustion Engines (ICE), Battery Energy Storage Systems (BESS), Photo-Voltaic panels (PV), PV Charge Controller (CHC) and Inverter/Rectifier (IR)

$CatCOMP = \{ICE, BESS, PV\}$: set of microgrid components selected from discrete catalog

CAT^x: set of models included in equipment catalog for component $x \in CAT$

$CAT = \bigcup_{x \in dCOMP} CAT^x$: set of all discrete models for components $x \in CAT$

J^x: set of expansion points for components $x \in \{ICE, BESS\}$ annuitization linear proxy

PARAMETERS:

$\hat{c}_i$: KiBaM *c* coefficient for BESS model $i \in CAT^{BESS}$

$\hat{C}_i^x$: unit / module cost of model $i \in CAT$ for component $x \in CatCOMP$

$\hat{C}_{diesel}$: diesel cost per liter

$\hat{C}_{mhrs}$: cost of single man hour

$\hat{C}^{NSE}$: cost of non-served energy

$\widehat{dr}$: discount rate

$\hat{E}_i^{mod}$: energy storage capacity of single module for BESS model $i \in CAT^{BESS}$

$\hat{H}_i^{min}$: minimum yearly up-time for ICE model $i \in CAT^{ICE}$

$\hat{k}_i$: KiBaM *k* coefficient for BESS model $i \in CAT^{BESS}$

$\widehat{LT}_i$: fixed lifetime of component / model $i \in CAT^{PV} \cup \{CHC, IR\}$

$\hat{m}^x$: slope of nominal power - investment cost curve for component $x \in \{CHC, IR\}$

$\hat{m}_i^F$: slope of power-fuel linear curve for ICE model $i \in CAT^{ICE}$

$\hat{m}_{i,j}^K$: slope of segment $j \in J^{ICE}$ of linear annuitization coefficient proxy for ICE model $i \in CAT^{ICE}$

$\hat{m}_{i,j}^{Kn}$: slope of plane $j \in J^{BESS}$ with respect to number of modules variable of linear equivalent annuitization coefficient proxy for BESS model $i \in CAT^{BESS}$

$\hat{m}_{i,j}^{KP}$: slope of plane $j \in J^{BESS}$ with respect to energy throughput variable of linear equivalent annuitization coefficient proxy for BESS model $i \in CAT^{BESS}$

$\hat{n}_t$: total number of simulation time-steps

$\hat{n}_i^{MAX,x}$: maximum number of installable modules of model $i \in CAT^x$ for component $x \in \{BESS, PV\}$

$\widehat{O\&M}_i^{\%}$: fraction of investment cost as yearly O&M for component / unit / module $i \in CAT \cup \{CHC, IR\}$

$\widehat{O\&M}_i^{mhr}$: yearly O&M required man-hours for component / unit / module $i \in CAT \cup \{CHC, IR\}$

$\hat{P}_i^{max}$: input at maximum load for ICE model $i \in CAT^{ICE}$

$\hat{P}_i^{min}$: input at minimum load for ICE model $i \in CAT^{ICE}$

$\hat{P}^{min,CHC}$: minimum *CHC* nominal power

$\widehat{PV}_{i,t}$: per-panel power production of PV model $i \in CAT^{PV}$ at time $t \in T$

$\hat{q}^x$: intercept of nominal power - investment cost curve for component $x \in \{CHC, IR\}$

$\hat{q}_i^F$: intercept of power-fuel linear curve for ICE model $i \in CAT^{ICE}$

$\hat{q}_{i,j}^K$: intercept of segment $j \in J^x$ of linear annuitization coefficient proxy for model $i \in CAT^x$ for component $x \in \{ICE, BESS\}$

$\widehat{R2I}^{ratio}$: nominal power ratio between inverter – rectifier sides of *IR*

$\widehat{SOC}_i^{min}/\widehat{SOC}_i^{max}$: minimum / maximum state of charge for BESS model $i \in CAT^{BESS}$

$\widehat{SU}_i^{pen}$: start-up consumption penalty for ICE model $i \in CAT^{ICE}$

$\widehat{\Delta D}^{\%}$: worst-case percentage demand increase in reserve scenario

$\widehat{\Delta P}_{PV}^{\%}$: worst-case percentage PV power output reduction in reserve scenario

REAL VARIABLES:

$Capex_i^x / Capex^y$: annuitized investment cost of model $i \in CAT^x$ for component $x \in CatCOMP, y \in \{CHC, IR\}$

$E_{i,t}$: energy content in BESS model $i \in CAT^{BESS}$ at time $t \in T$

$E_{i,t}^1$: readily available energy content in BESS model $i \in CAT^{BESS}$ at time $t \in T$

$E_{i,t}^2$: bounded energy content in BESS model $i \in CAT^{BESS}$ at time $t \in T$

$F_{i,t}$: fuel consumption of ICE $i \in CAT^{ICE}$ at time $t \in T$

$K_i^{eq,BESS}$: linearized proxy of equivalent annuitization coefficient for BESS $i \in CAT^{BESS}$

K_i^{ICE}: linearized proxy of annuitization coefficient for ICE $i \in CAT^{ICE}$

n_i^x: number of installed modules of model $i \in CAT^x$ for component $x \in \{BESS, PV\}$

$Opex_i^x / Opex^y$: yearly overall operation and maintenance cost of model $i \in CAT^x$ for component $x \in CatCOMP, y \in \{CHC, IR\}$

$P_{i,t}^x$: power output of model $i \in CAT^x$ for component $x \in \{ICE, PV\}$ at time $t \in T$

$P_{i,t}^{BESS\rightarrow} / P_{i,t}^{BESS\leftarrow}$: outward / inward power flow from BESS model $i \in CAT^{BESS}$ at time $t \in T$

$P_t^{BESS,res}$: overall spinning reserve contribution of BESS systems at time $t \in T$

P_t^{inv} / P_t^{rect}: DC to AC / AC to DC power flow through *IR* at time $t \in T$

$P^{nom,X}$: nominal power of component $x \in \{CHC, IR\}$

$P_t^{PV,res}$: worst-case power production from PV systems at time $t \in T$

BINARY VARIABLES:

I_i^x / I^y: investment variable of model $i \in CAT^x$ for component $x \in CatCOMP, y \in \{CHC, IR\}$

$Z_{i,t}$: on-off variable of ICE model $i \in CAT^{ICE}$ at time $t \in T$

$\delta_{i,t}$: start-up variable of ICE model $i \in CAT^{ICE}$ at time $t \in T$

OBJECTIVE FUNCTION:

$$\min \sum_{x \in CatCOMP} \sum_{i \in CAT^x} (Capex_i^x + Opex_i^x) + \sum_{x \in \{CHC, IR\}} (Capex^x + Opex^x) + \sum_{t \in T} \pi_t \cdot \hat{C}^{NSE}$$

ICE CONSTRAINTS:

ICE max-min power output:

$\hat{P}_i^{min} \cdot Z_{i,t} \leq P_{i,t}^{ICE} \leq \hat{P}_i^{max} \cdot Z_{i,t} \quad \forall\, i \in CAT^{ICE}, t \in T$

ICE start-up variable:

$\delta_{i,t} \geq Z_{i,t} - Z_{i,t-1} \quad \forall\, i \in CAT^{ICE}, t \in T$

ICE fuel consumption curve:

$F_{i,t} = \hat{m}_i^F \cdot P_{i,t}^{ICE} + \hat{q}_i^F \cdot Z_{i,t} \quad \forall\, i \in CAT^{ICE}, t \in T$

Minimum ICE yearly up-time:

$\sum_{t \in T} Z_{i,t} \cdot \frac{8760}{\hat{n}_t} \geq \hat{H}_i^{min} \cdot I_i^{ICE} \quad \forall\, i \in CAT^{ICE}, t \in T$

ICE investment decision:

$\sum_{t \in T} Z_{i,t} \leq I_i^{ICE} \cdot \hat{n}_t \quad \forall\, i \in CAT^{ICE}$

ICE annualization coefficient linearization:

$K_i^{ICE} \geq \hat{m}_j^K \cdot \sum_{t \in T} Z_{i,t} + \hat{q}_j^K \cdot I_i^{ICE} \quad \forall\, i \in CAT^{ICE}, j \in J$

Annuitized ICE investment cost:

$Capex_i \geq \hat{C}_i^{ICE} \cdot K_i^{ICE} - (1 - I_i^{ICE}) \cdot \hat{C}_i^{ICE} \quad \forall\, i \in CAT^{ICE}$

ICE operating cost:

$$Opex_i = \sum_{t\in T}\left(F_{i,t} + \delta_{i,t}\cdot SU_i^{pen}\right)\cdot\frac{8760}{\hat{n}_t} + \left(\hat{C}_i^{ICE}\cdot\widehat{O\&M}_i^{\%} + \widehat{O\&M}_i^{mhrs}\cdot\hat{C}_{mhrs}\right)\cdot I_i^{ICE} \qquad \forall\, i\in CAT^{ICE}$$

BESS CONSTRAINTS:

BESS charge / discharge power:

$$P_{i,t}^{BESS\leftarrow}, P_{i,t}^{BESS\rightarrow} \geq 0 \qquad \forall\, i\in CAT^{BESS}, t\in T$$

KiBaM power constraints:

$$P_{i,t}^{BESS\leftarrow} \leq \frac{\hat{c}_i\cdot n_i^{BESS}\cdot\hat{E}_i^{mod} + E_{i,t}^1\cdot e^{-\hat{k}_i} + E_{i,t}\cdot\hat{c}_i\cdot\left(1-e^{-\hat{k}_i}\right)}{\frac{1}{\hat{k}_i}\left(1-e^{-\hat{k}_i} + \hat{c}_i\cdot\left(\hat{k}_i + e^{-\hat{k}_i} - 1\right)\right)}$$

$$P_{i,t}^{BESS\rightarrow} \leq \frac{E_{i,t}^1\cdot\hat{k}_i\cdot e^{-\hat{k}_i} + E_{i,t}\cdot\hat{c}_i\cdot\hat{k}_i\cdot\left(1-e^{-\hat{k}_i}\right)}{\left(1-e^{-\hat{k}_i} + \hat{c}_i\cdot\left(\hat{k}_i + e^{-\hat{k}_i} - 1\right)\right)} \qquad \forall\, i\in CAT^{BESS}, t\in T$$

KiBaM total energy / available energy / bounded energy evolution:

$$E_{i,t+1} = E_{i,t} + P_{i,t}^{BESS\leftarrow} - P_{i,t}^{BESS\rightarrow} \qquad \forall\, i\in CAT^{BESS}, t\in T$$

$$E_{i,t+1}^1 = E_{i,t}^1\cdot e^{-\hat{k}_i} + E_{i,t}\cdot\hat{c}_i\cdot\left(1-e^{-\hat{k}_i}\right) + E_{i,t+1}\cdot\frac{1}{\hat{k}_i}\left(1-e^{-\hat{k}_i} + \hat{c}_i\cdot\left(\hat{k}_i + e^{-\hat{k}_i} - 1\right)\right)$$

$$E_{i,t}^2 = E_{i,t} - E_{i,t}^1$$

BESS capacity limits:

$$n_i^{BESS}\cdot\hat{E}_i^{mod}\cdot\widehat{SOC}_i^{min} \leq E_{i,t} \leq n_i^{BESS}\cdot\hat{E}_i^{mod}\cdot\widehat{SOC}_i^{max} \qquad \forall\, i\in CAT^{BESS}, t\in T$$

BESS reserve power:

$$P_t^{BESS,res} \leq \sum_{i\in CAT^{BESS}}\frac{E_{i,t}^1\cdot\hat{k}\cdot e^{-\hat{k}} + E_{i,t}\cdot\hat{c}\cdot\hat{k}\cdot\left(1-e^{-\hat{k}}\right)}{\left(1-e^{-\hat{k}} + \hat{c}\cdot\left(\hat{k} + e^{-\hat{k}} - 1\right)\right)} \qquad \forall\, t\in T$$

$$P_t^{BESS,res} \leq \sum_{i\in CAT^{BESS}}\left(E_{i,t} - n_i^{BESS}\cdot\hat{E}_i^{mod}\cdot\widehat{SOC}_i^{min}\right) \qquad \forall\, t\in T$$

BESS investment decision:

$$n_i^{BESS} \leq \hat{n}_i^{MAX}\cdot I_i^{BESS} \qquad \forall\, i\in CAT^{BESS}$$

BESS equivalent annualization coefficient linearization (includes number of modules):

$$K_i^{eq,BESS} \geq \widehat{m}_{j'}^{KP}\cdot\sum_{t\in T}\left(P_{i,t}^{BESS\rightarrow} + P_{i,t}^{BESS\leftarrow}\right) + \widehat{m}_{j'}^{Kn}\cdot n_i^{BESS} + \hat{q}_{j'}^{K}\cdot I_i^{BESS} \qquad \forall\, i\in CAT^{BESS}, j'\in J'$$

Annuitized BESS investment cost:

$$Capex_i^{BESS} \geq \hat{C}_i^{BESS}\cdot K_i^{eq,BESS} \qquad \forall\, i\in CAT^{BESS}$$

BESS operating cost:

$$Opex_i^{BESS} = \hat{C}_i^{BESS}\cdot n_i^{BESS}\cdot\widehat{O\&M}_i^{\%} + \widehat{O\&M}_i^{mhrs}\cdot\hat{C}_{mhrs}\cdot I_i \qquad \forall\, i\in CAT^{BESS}$$

PV CONSTRAINTS:

PV power production:

$$P_{i,t}^{PV} \leq \widehat{PV}_{i,t}\cdot n_i^{PV}\ \forall\, i\in CAT^{PV}, t\in T$$

PV reserve production:

$$P^{PV,res} \leq \sum_{i\in CAT^{PV}}\left(\widehat{PV}_{i,t}\cdot n_i^{PV}\right)\left(1-\widehat{\Delta P}_{PV}^{\%}\right) \qquad \forall\, i\in CAT^{PV}, t\in T$$

PV investment decision:

$$n_i^{PV} \leq \hat{n}_i^{MAX}\cdot I_i \qquad \forall\, i\in CAT^{PV}$$

Annuitized PV investment cost:

$$Capex_i^{PV} = \frac{\hat{C}_i^{PV}\cdot n_i^{PV}\cdot\widehat{dr}}{1-\left(1+\widehat{dr}\right)^{-LT_i}} \qquad \forall\, i\in CAT^{PV}$$

PV operating cost:

$$Opex_i^{PV} = \hat{C}_i^{PV}\cdot n_i^{PV}\cdot\widehat{O\&M}_i^{\%} + \widehat{O\&M}_i^{mhrs}\cdot\hat{C}_{mhrs}\cdot I_i^{PV} \qquad \forall\, i\in CAT^{PV}$$

INVERTER/RECTIFIER CONSTRAINTS:

Inverter – Rectifier (IR) power:

$P_t^{inv}, P_t^{rect} \geq 0 \quad \forall\, t \in T$

Nominal IR power:

$P^{nom,IR} \geq P_t^{inv} \cdot \eta^{inv} \qquad \forall\, t \in T$

$P^{nom,IR} \geq \frac{P_t^{rect}}{\widehat{RRI}^{ratio}}$

IR investment decision:

$I^{IR} \cdot (|CAT^{BESS}| + |CAT^{PV}|) \geq \sum_{i \in CAT^{PV}} I_i^{PV} + \sum_{i \in CAT^{BESS}} I_i^{BESS}$

Annuitized IR investment cost:

$Capex^{IR} = \frac{(\hat{m}^{IR} \cdot P^{nom,IR} + \hat{q}^{IR} \cdot I^{IR}) \cdot \widehat{dr}}{1-(1+\widehat{dr})^{-LT^{IR}}}$

IR operating cost:

$Opex^{IR} = (\hat{m}^{IR} \cdot P^{nom,IR} + \hat{q}^{IR} \cdot I^{IR}) \cdot \widehat{O\&M}_i^{\%} + \widehat{O\&M}_i^{mhrs} \cdot \hat{C}_{mhrs} \cdot I^{IR}$

PV CHARGE CONTROLLER CONSTRAINTS:

Charge Controller (CHC) nominal power:

$P^{nom,CHC} \geq P_{i,t}^{PV} \cdot \hat{\eta}^{CHC} \qquad \forall\, i \in CAT^{PV}, t \in T$

Minimum CHC size:

$P^{nom,CHC} \geq \hat{P}^{min,CHC} \cdot I_i^{PV} \qquad \forall\, i \in CAT^{PV}$

Annuitized CHC investment cost:

$Capex^{CHC} = \frac{\left(\hat{m}^{CHC} \cdot P^{nom,CHC} + \sum_{i \in CAT^{PV}} I_i^{PV} \cdot \hat{q}^{CHC}\right) \cdot \widehat{dr}}{1-(1+\widehat{dr})^{-LT^{CHC}}}$

CHC operating cost:

$Opex^{CHC} = \left(\hat{m}^{CHC} \cdot P_i^{nom,CHC} + \sum_{i \in CAT^{PV}} I_i^{PV} \cdot \hat{q}^{CHC}\right) \cdot \widehat{O\&M}_i^{\%} + \widehat{O\&M}_i^{mhrs} \cdot \hat{C}_{mhrs} \cdot \sum_{i \in CAT^{PV}} I_i^{PV}$

ENERGY BALANCES AND SPINNING RESERVE:

DC-bus balance:

$\sum_{i \in CAT^{BESS}} \left(P_{i,t}^{BESS\rightarrow} \hat{\eta}_i^{BESS\rightarrow} - \frac{P_{i,t}^{BESS\leftarrow}}{\hat{\eta}_i^{BESS\leftarrow}} \right) + \sum_{i \in CAT^{PV}} \left(P_{i,t}^{PV} \hat{\eta}^{CHC} \right) - P_t^{inv} + P_t^{rect} \hat{\eta}^{rect} = 0 \quad \forall\, t \in T$

AC-bus balance:

$\sum_{i \in CAT^{ICE}} P_{i,t}^{ICE} + P_t^{inv} \hat{\eta}^{inv} - P_t^{rect} = \left(\widehat{D}_t - \pi_t\right)(1 + \hat{\eta}^{distr})$

Spinning reserve constraint:

$\sum_{i \in CAT^{ICE}} \hat{P}_i^{max} Z_{i,t} + P_t^{BESS,res} \hat{\eta}_i^{BESS\rightarrow} \hat{\eta}^{inv} \geq \left(1 + \widehat{\Delta D}^{\%}\right)\left(\widehat{D}_t - \pi_t\right) - P_t^{PV,res} \hat{\eta}^{CHC} \hat{\eta}^{inv}$

SINGLE ICE—BESS—PV ARCHITECTURE:

$\sum_{i \in CAT^x} I_i \leq 1 \quad \forall\, x \in CatCOMP$